Bioactive Materials 13 (2022) 149–160

Contents lists available at ScienceDirect

Bioactive Materials

journal homepage: www.keaipublishing.com/en/journals/bioactive-materials

Dominant role of *in situ* native cartilage niche for determining the cartilage type regenerated by BMSCs

Mengjie Hou [a,b,1], Baoxing Tian [d,1], Baoshuai Bai [b,c,1], Zheng Ci [b,c], Yu Liu [b,c], Yixin Zhang [a], Guangdong Zhou [a,b,c,**], Yilin Cao [a,b,*]

[a] Department of Plastic and Reconstructive Surgery, Shanghai 9th People's Hospital, Shanghai Jiao Tong University School of Medicine, Shanghai Key Laboratory of Tissue Engineering, Shanghai, PR China
[b] National Tissue Engineering Center of China, Shanghai, PR China
[c] Research Institute of Plastic Surgery, Wei Fang Medical College, Weifang, PR China
[d] Department of Breast Surgery, Tongren Hospital, Shanghai Jiao Tong University School of Medicine, Shanghai, 200336, PR China

ARTICLE INFO

Keywords:
BMSCs
Niche
Cartilage type
Cartilage regeneration
In situ
Chondrocytes

ABSTRACT

Tissue-engineered cartilage regeneration by bone marrow stromal cells (BMSCs) is considered an ideal method. However, how to regulate BMSCs to regenerate specific types of cartilage remains unclear, which significantly limits its clinical translation and leads to suboptimal clinical effects. Herein, we systematically explored the role of native ear and articular cartilage niches on the differentiation fate of BMSCs and the type of regenerated cartilage. First, we prepared two types of acellular cartilage sheets (ACSs) and two types of chondrocytes. Then green fluorescent protein-labeled BMSCs were seeded on two types of ACSs with or without corresponding types of chondrocytes using a sandwich model and directed or cross-implanted them into native cartilage niches. After one year of *in vivo* culture, cell tracking and the results of histological results showed that the native cartilage niches were capable of regulating BMSCs regeneration into specific types of cartilage that were consistent with the cartilage types of the implanted sites. Furthermore, even when the type of niche formed by ACSs or the biomimetic cartilage niche constructed by specific types of ACSs and specific types of chondrocytes did not match with the native cartilage niche, the native cartilage niche continued to determine the type of cartilage regenerated by implanted BMSCs and chondrocytes. All our results provide sufficient evidence for specific types of cartilage regeneration using chondrogenic potential cells, such as mesenchymal stem cells and chondrocytes.

1. Introduction

Cartilage exhibits poor self-repair capacity owing to the lack of vasculature and nerves [1], which makes the repair of cartilage defects a clinical problem. Tissue engineering is a promising method for regenerating cartilage by combining proper scaffolds with suitable seed cells [2–4]. As the core element of tissue engineering, finding an appropriate source of seed cells remains a significant challenge that has restricted the clinical translation of tissue-engineered cartilage regeneration technology. Chondrocytes, bone marrow stromal cells (BMSCs), and adipose stem cells have been widely reported to be used for cartilage regeneration, and even partially achieve clinical translation [5–7]. BMSCs are considered as relatively ideal seed cells for cartilage regeneration owing to several properties, such as multi-directional differentiation, the ability to induce less trauma at the donor sites, wide sources, and strong proliferation capacity, and these properties have been fully demonstrated via the *in vitro* regeneration of mature cartilage and repair of cartilage defects *in vivo* [8–10].

However, cartilage can be characterized into three subtypes: elastic cartilage (such as ear cartilage), hyaline cartilage (such as articular

Peer review under responsibility of KeAi Communications Co., Ltd.
* Corresponding author. Shanghai Key Lab of Tissue Engineering, Shanghai 9th People's Hospital, Shanghai Jiao Tong University School of Medicine, No. 639 Zhi Zao Ju Road, Shanghai, 200011, PR China.
** Corresponding author. Shanghai Key Lab of Tissue Engineering, Shanghai 9th People's Hospital, Shanghai Jiao Tong University School of Medicine, Shanghai, 200011, PR China.
E-mail addresses: guangdongzhou@126.com (G. Zhou), yilincao@yahoo.com (Y. Cao).
[1] These authors contributed equally to this work.

https://doi.org/10.1016/j.bioactmat.2021.11.007
Received 20 August 2021; Received in revised form 3 November 2021; Accepted 4 November 2021
Available online 12 November 2021

cartilage and costal cartilage), and fibrocartilage (such as meniscus and intervertebral disc) [11–13]. At present, few studies have reported whether BMSCs could be regulated to regenerate specific types of cartilage. Moreover, the three types of cartilage demonstrate distinct biological functions owing to their different structures. For instance, ear cartilage expresses abundant elastin, resulting in strong elasticity and resilience [14–16]. Articular cartilage expresses PRG4, also known as lubricin, which prevents cartilage wear caused by joint movement [17–19]. Therefore, methods for regulating BMSCs to regenerate specific types of cartilage for accurate cartilage regeneration and long-term functional reconstruction are urgently needed for clinical translation [20].

Previous studies have demonstrated that BMSCs induced by chondrocytes (co-culture), biomimetic scaffolds, and chondrogenic medium system can achieve cartilage regeneration *in vitro* [21–23], and can also repair articular cartilage defects [24–26]. However, these studies mainly focused on BMSC regenerated cartilage (BRC), which possesses cartilage extracellular matrix (ECM) deposition, including glycosaminoglycans (GAG) and type II collagen (COL II), to be observed in all three types of cartilage; however, the examination of the type of BRC has garnered little interest. Furthermore, Sun et al. described hyaline-like cartilage regeneration for injured articular cartilage using dual-factor-releasing BMSC-laden hydrogels and physically gradient synthetic biodegradable polymers [27]. Kang et al. also demonstrated the formation of an engineered, anatomical analog of osteochondral tissue with lubricin-positive cartilage formation in the articular cartilage niche by combining a trilayer scaffold with BMSCs [28]. However, due to the lack of identification of specific indicators for the three types of cartilage and the lack of cell labeling and tracking, the type of BRC regulated by the native articular cartilage niche could not be determined. More importantly, the regulatory role of other types of native cartilage niches (such as elastin cartilage niche) on BRC types remains poorly understood. Therefore, systematic research investigating with the type of the differentiation of BMSC into specific types of cartilage is lacking. The following critical issues need to be examined: 1) whether specific types of cartilage niches can regulate BMSCs to regenerate specific types of cartilage; 2) whether the niche provided by scaffolds affects the regulation of the type of BRC by the native cartilage niche; and 3) in case of a conflict between specific biomimetic types of cartilage niches and the native cartilage niche, which of these controls the ultimate type of BRC needs to be determined.

To address these issues, in the current study, we used a previously established technology to prepare two types of acellular cartilage sheets (ACSs) (ear and articular) that retained specific structures and components of cartilage [29]. Subsequently, green fluorescent protein (GFP)-labeled BMSCs were seeded on the specific types of ACSs with or without specific types of chondrocytes using a sandwich model [29] to provide BMSCs with biomimetic cartilage niches that matched or mismatched with the native cartilage niche types. Thereafter, the engineered constructs were directed or cross-implanted into specific types of native cartilage niches as follows: 1) niche-matched group: BMSC-ear ACS (EACS) constructs implanted into the ear cartilage niche and BMSC-articular ACS (AACS) constructs implanted into the articular cartilage niche, 2) ACS niche mismatched group: BMSC-AACS constructs implanted into the ear cartilage niche and BMSC-EACS constructs implanted into the articular cartilage niche, 3) biomimetic niche mismatched group: BMSC-AACS-articular chondrocyte (ARC) constructs implanted into the ear cartilage niche and BMSC-EACS-ear chondrocyte (EAC) constructs implanted into the articular cartilage niche. Finally, cell tracking analysis and the identification of specific types of cartilage were performed to elucidate the types of BRC in the aforementioned groups and to identify the determining factor that determines the type of BRC.

2. Materials and methods

2.1. Animal information

A total of 12 four-month-old hybrid pigs (six male and six female; Yangtze River Delta White pig; Shanghai Jiagan Biological Technology Co., Shanghai, China) weighing 25–30 kg were used in this study. All animal experiments were approved by Animal Experimental Ethical Committee of Shanghai Ninth People's Hospital (HKDL [2016].76), affiliated to Shanghai Jiao Tong University school of medicine. All experiments were conducted by the Key Laboratory of Tissue Engineering at Shanghai Ninth People's Hospital.

2.2. Preparation of the two types of ACSs

Ear and articular ACSs were prepared as described previously [29,30]. Briefly, ear and articular cartilage harvested from adult pigs were drilled using corneal trephine into a circular cylinder with a diameter of 7 mm, and cartilage sheets with a thickness of 10 μm were obtained via frozen sectioning. After decellularization with 1% sodium dodecyl sulfate (SDS, Solarbio, Beijing, China) for 24 h, the sheets were rinsed thrice with sterile water and then lyophilized in a vacuum freeze-drier (Virtis Benchtop 6.6; SP Industries, Gardiner, NY).

2.3. Characterization of ACSs

The morphology of the ear and articular cartilage sheets before and after decellularization was first observed using scanning electron microscopy (SEM, JEOL JSM-5600LV, Kyoto, Japan) [29]. For histological analysis, 4,6-diamidino-2-phenylindole (DAPI, Sigma-Aldrich, USA) and hematoxylin and eosin (HE) staining were performed to observe the nucleus, and Safranin O (SO) was used to detect the deposition of GAG. For immunohistochemical analysis, a rabbit polyclonal antibody against Col II (1:100 in PBS; ab34712, Abcam, Cambridge, MA, USA) was used to detect the expression of Col II, followed by incubated with an HRP-conjugated anti-rabbit secondary antibody (1:100; Dako, Glostrup, Denmark). Diaminobenzidine tetrahydrochloride (DAB, Santa Cruz Biotechnology) was used to develop color, thereby aiding visualization, according to a previously established method [31].

Cartilage sheets were weighed before and after decellularization for the quantitative analysis of DNA, GAG and total collagen using the Quant-iT Pico-Green dsDNA kit (Invitrogen), dimethyl methylene blue assay kit (Sigma-Aldrich), and hydroxyproline (HYP) assay kit (Sigma-Aldrich), respectively according to previously described methods [32–34].

The Young's modulus of scaffolds was analyzed using a Nanoindenter (Piuma nanoindenter, Optics11 BV, Netherlands) equipped with a spherical probe. The method used in this study was similar to that described previously [35,36]. For all indentations, probe stiffness, probe radius, and indentation velocity (loading rate) were set to 0.48 N/m, 254 μm, and 5 μm/s, respectively. Nanoindentations were performed at 10 indentation sites on each sample. The Young's Modulus of all samples was calculated using a Hertzian model based on 80% of the data on the loading section of the load-indentation data curve ($n = 6$).

2.4. Isolation and culture of BMSCs and chondrocytes

The bone marrow was aspirated from the anterior superior iliac spine of healthy pigs. BMSCs were isolated and cultured in regular culture medium composed of low-glucose Dulbecco's Modified Eagle Medium (DMEM, Gibco BRL, Grand Island, NY) and 10% fetal bovine serum (FBS, Hyclone, Logan, UT, USA) according to previously established methods [22,37]. Chondrocytes isolated from the ear and articular cartilage were harvested and cultured in regular culture medium (high-glucose DMEM, 10%FBS) as previously described [38].

2.5. Biocompatibility evaluation of the ACSs

2.5.1. Cellular attachment and cell seeding efficiency for ACSs

A total of 20×10^6 BMSCs in 1.0 ml of regular culture medium were evenly dropped onto the EACSs and AACSs. BMSC-EACS-EAC and BMSC-AACS-ARC constructs were prepared in the same manner. The ratio of BMSCs to chondrocytes was 6:4, and the final seeding concentration was 20×10^6 cells/ml. The cell-ACS constructs were then incubated to allow for the complete adhesion of the cells to the ACSs. After 24 h of incubation, the cell-ACS constructs were gently transferred into a new 6-well plate. The remaining cells from the different groups were collected, and the cell number was counted. The cell seeding efficiency of the samples was calculated based on the following formula: (total cell number − remaining cell number)/total cell number × 100%, to evaluate the adherent ability of cells on the EACSs and AACSs. After 3 days of culture, ACSs with or without cells were fixed overnight in 0.05% glutaraldehyde at 4 °C. After dehydration in a graded ethanol series, samples were subjected to critical-point drying, and the attachment of cells on the ACSs was examined using SEM.

2.5.2. Cell viability on the ACSs

After 1, 4, and 7 days of culture, the viabilities of BMSCs and chondrocytes on ACSs were determined using the Live & Dead Cell Viability Assay (Invitrogen, USA) following the manufacturer's instructions. The cells were examined using a confocal microscope (Nikon, Japan).

2.6. Labeling of BMSCs

To trace the distribution and differentiation of BMSCs after implantation *in vivo*, we labeled BMSCs with GFP via lentivirus transfection (LV-CMV > EGFP/T2A/Puro, Cyagen, China) at a multiplicity of infection (MOI) of 40. Briefly, after reaching 30–40% confluence at passage 1, BMSCs were incubated with lentivirus in regular culture medium for 16 h at 37 °C. The culture medium was replaced with the fresh medium followed by incubation for another 24 h. Thereafter, in order to improve the infection efficiency of lentivirus for BMSCs, puromycin (HY–B1743A, MedChemExpress, China) was then incubated with BMSCs at a concentration of 3 μg/ml in the regular culture medium until all unlabeled BMSCs were killed. All labeled BMSCs at passage 3 were prepared for subsequent experiments.

The efficiency of lentiviral transfection of BMSCs was analyzed using confocal laser scanning microscopy (TCS SP8 STED 3X, Leica, Germany) [39] and flow cytometry as reported previously [40,41]. Moreover, the cell proliferation of labeled and unlabeled BMSCs was further evaluated using the CCK-8 assay (Dojindo Molecular Technologies, Kumamoto, Japan) after *in vitro* culturing for 1, 3, 5, and 7 days [42].

2.7. Engineering of cell-ACS constructs and implantation

2.7.1. In vitro construction and in vivo implantation of the niche matched group

BMSC-EACS and BMSC-AACS constructs were engineered using the previously established sandwich model [29,30]. Briefly, GFP-labeled BMSCs were harvested at passage 3 and suspended in regular culture medium at a final concentration of 8×10^7 cells/ml. Next, a piece of ACS was placed in a culture dish and seeded with 5 μl of BMSC suspension. Another piece of ACS was then stacked on top of the first, followed by seeding with the same amount of the cell suspension. The aforementioned procedure was repeated until ACSs formed 20 layers, followed by 4 h of incubation in culture dishes. Subsequently, all constructs were cultured in regular culture medium for 3 days *in vitro* before *in vivo* implantation.

After anesthesia, preoperative skin preparation, and disinfection, the area between the ear cartilage or the area between the perichondrium and cartilage was separated at the dorsal ear to form a pocket of sufficient size. Two BMSC-EACS constructs were stacked together and implanted into the same separated area (n = 6 pigs). Subsequently, the upper and lower edges of the cartilage or perichondrium at the incision were sutured with biodegradable sutures to fix the constructs in a closed space. Thereafter, BMSC-AACS constructs were immediately implanted into the *in situ* articular cartilage niche of the same pig, as previously described [43]. Briefly, cylindrical defects (6 mm diameter, 3 mm depth) were created using a trephine at the weight-bearing area of the lateral condyles of the knee joint. After the elimination of the blood clots, each defect was repaired with BMSC-AACS constructs (two constructs from the same group were stacked together and implanted at the same defect site) (n = 6 pigs). Constructs were fixed in place by stitching the surrounding native cartilage with biodegradable sutures.

2.7.2. In vitro construction and in vivo implantation of scaffold niche mismatched group

After the BMSC-ACS constructs were implanted into cartilage niches of the same type as their ACS, they were also cross-implanted into different types of cartilage niches of the same pig. Using the same surgical procedure, the BMSC-AACS constructs were implanted into the ear cartilage niche, and the BMSC-EACS constructs were implanted into the articular cartilage defects.

2.7.3. In vitro construction and in vivo implantation of biomimetic cartilage niche mismatched group

GFP-labeled BMSCs at passage 3 and chondrocytes (ear and articular) at passage 2 were harvested. BMSC-EACS-EAC and BMSC-AACS-ARC constructs were prepared in the same manner. The ratio of BMSCs to chondrocytes was 6:4, and the final seeding concentration was 8×10^7 cells/ml. As shown in Fig. 1, after culturing under *in vitro* conditions for 3 days, the BMSC-EACS-EAC constructs were implanted into the *in vivo* articular cartilage defects (n = 6 pigs), whereas the BMSC-AACS-ARC constructs were implanted into the area between the ear cartilage or the area between the perichondrium and ear cartilage (n = 6 pigs).

2.8. Detection of GFP-labeled cells in regenerated tissues

After 1 year of *in vivo* culturing, BMSC-regenerated tissues (n = 6 pigs) were collected. Gross images were captured, and tissues were fixed in 4% paraformaldehyde (PFA) at 4 °C overnight. Next, all samples were treated sequentially with 10%, 20%, and 30% sucrose solution for dehydration, and the sucrose solutions were dehydrated for 24 h to ensure complete dehydration. After washing thrice with PBS, the samples were frozen in OCT gel (Sakura), sliced into sections with a thickness of 8 μm, and stained with DAPI for observing the nuclei. The distribution and location of GFP-positive cells in the regenerated tissues were observed using confocal laser scanning microscopy. The chondrogenic differentiation type of labeled cells was further analyzed using histological and immunohistochemical analysis.

2.9. Histological and immunohistochemical analysis

To evaluate the type of BRC in specific types of native cartilage niches, all engineered tissues harvested above were subjected to histological and immunohistochemical examinations. HE, Safranin-O/Fast Green (SO/FG) staining, and immunohistochemical staining of type II collagen were performed to observe the histological structure and cartilage matrix deposition of GAG and COL II, respectively [44]. An Elastin Stain kit (ab150667, Abcam) was used to detect the expression of elastin (a specific protein of elastin cartilage), according to the manufacturer's protocol. In addition, PRG4 (a specific protein of articular cartilage) (ab94933, Abcam) and α-SMA (a specific protein of fibrocartilage) were detected using immunohistochemical staining as per the manufacturer's protocols [17]. Furthermore, the expression levels of various proteins in BRC were measured using Image J software to

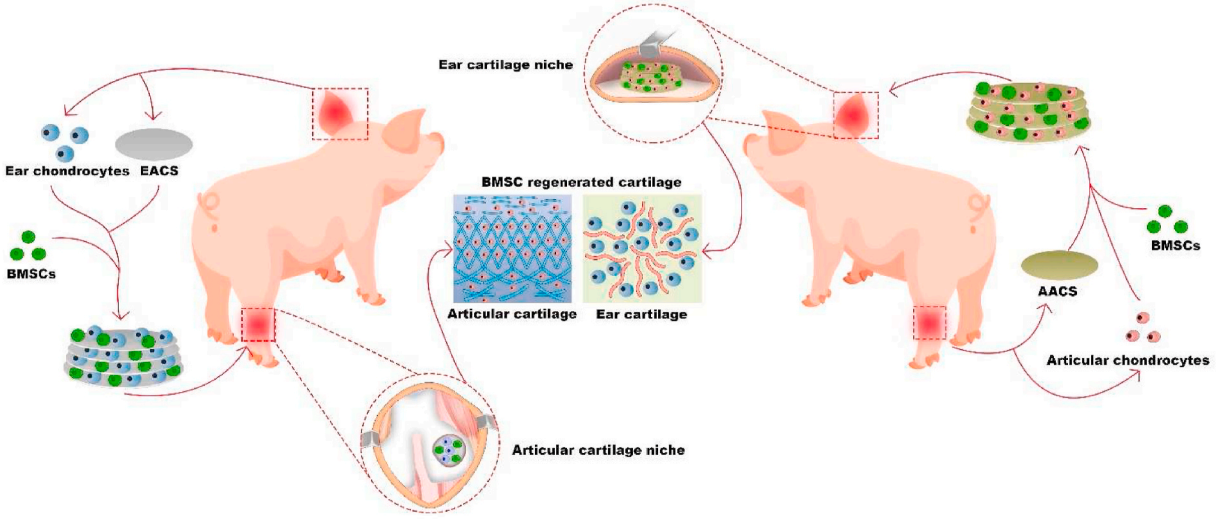

Fig. 1. Schematic description of the study design. BMSCs were seeded on specific types of acellular cartilage sheets (ACSs) with specific types of chondrocytes using a sandwich model. The engineered constructs were cross-implanted into specific types of native cartilage niches for 1 year. The results confirmed that when the types of niches provided by the biomimetic cartilage niche constructed by specific types of ACSs and specific types of chondrocytes did not match with the native cartilage niches, the *in situ* ear and articular cartilage niches regulated BMSC regeneration of ear and articular cartilage, respectively, which was consistent with the native cartilage type of the implanted site. Abbreviations: BMSCs, bone marrow stromal cells, EACS, ear acellular cartilage sheet; AACS, articular acellular cartilage sheet.

quantitatively analyze the staining results [45,46]. The IHC profiler plug-in was used to automatically score the staining of the sample based on the staining intensity and extent of positive staining. The staining intensity was reported as the optical density value of the images, which was evaluated through deconvolution using the IHC profiler plugin in Image J. Subsequently, the staining area was scored according to the percentage contribution of the positive staining area: 0 (0–10%), 1 (10–20%), 2 (20–40%), 3 (40–70%), and 4 (>70%). Finally, the sum of the staining intensity and the positive extent score of the staining, also known as the IHC score, was calculated and defined as follows: high positive (3+), positive (2+), low positive (1+), negative (0–1). The IHC score was generated from four different quadrants of the slides, and the average score for each sample was calculated.

2.10. Real-time quantitative polymerase chain reaction (RT-qPCR) analysis

RT-qPCR was performed to determine the expression of chondrogenesis-related genes (*SOX9*, *aggrecan*, and *COL II*) and specific types of cartilage-related genes (*elastin*, *PRG4*, and *α-SMA*) using *β-actin* as the reference gene for BRC [47]. The chondrocytes were first isolated from regenerated cartilage samples, and harvested in regular culture media. Next, flow cytometry was used to sorted the GFP-positive chondrocytes among all harvested cells, and verify the proportion of GFP-positive cells in the sorted cells. Thereafter, the sorted cells were further analyzed by RT-qPCR. Briefly, total RNA was extracted from the sorted GFP-positive cells and native cartilage (ear and articular cartilage) using TRIzol reagent (Invitrogen, Carlsbad, CA), and the RNA concentration was determined using a Nanodrop 2000 spectrophotometer (Thermo Fisher Scientific, Waltham, MA, USA). Reverse transcription (RT) was performed to obtain cDNA using M-MLV 5 × Reaction Buffer (Promega, Madison, WI, USA), according to previously described methods. RT-qPCR was performed using the SYBR Premix Ex TaqTM II (Takara, Kyoto, Japan), and the results were analyzed using an Applied Biosystems AB instrument (Foster City, CA). All tests were performed in triplicate, normalized relative to the expression of housekeeping gene *β-actin*, and analyzed using the $2^{-\Delta Ct}$ method. The primer sequences are listed in Table S1.

2.11. Statistical analysis

All quantitative data are presented as the mean ± standard deviation. Data were analyzed using GraphPad Prism 5.0, and a one-way ANOVA test was used to analyze statistical differences between the groups. The results of the quantitative analysis of DNA, GAG, HYP, and Young's modulus content of cartilage sheets before decellularization were compared to those obtained after decellularization. The histological scores and expression levels of genes in regenerated cartilage (RC) were compared with those of native cartilage (NC). Results were considered statistically significant at $p < 0.05$.

3. Results

3.1. Characterizations of ACSs

Ear and articular cartilage sheets with a thickness of 10 μm were obtained by frozen sectioning. As shown in Fig. 2A, the articular cartilage sheets appeared to be more transparent than the ear cartilage sheets, as demonstrated by gross images. After being decellularized, spread out, and freeze-dried, ACSs showed an appearance more similar to that of native cartilage; hence, the EACSs appeared ivory white, and the AACSs appeared transparent. In addition, ACSs demonstrated a minor shape distortion after freeze-drying, which was attributed to their low thinness (Fig. 2A). The two types of ACSs were almost completely clear of all cellular components, as revealed by SEM (Fig. 2B), DAPI staining (Fig. 2C), and HE staining (Fig. 2D); the results were confirmed by DNA content analysis (Fig. 2G). More importantly, SEM images and HE staining also showed that both EACSs and AACSs had specific surface topological structure, which were consistent with those of the native ear cartilage and articular cartilage, respectively (Fig. 2B, D). Furthermore, SO staining (Fig. 2E) and immunohistochemical analysis of COL II (Fig. 2F) indicated that the ear and articular ACSs retained most of the cartilage-specific ECM (GAG and COL II) components, as confirmed by the quantitative analysis of GAG and hydroxyproline (HYP) (Fig. 2H and I). The mechanical properties of different scaffolds were then evaluated. The results of Young's modulus revealed that the ACSs still preserved part of the mechanical properties of the native cartilage (Fig. 2J).

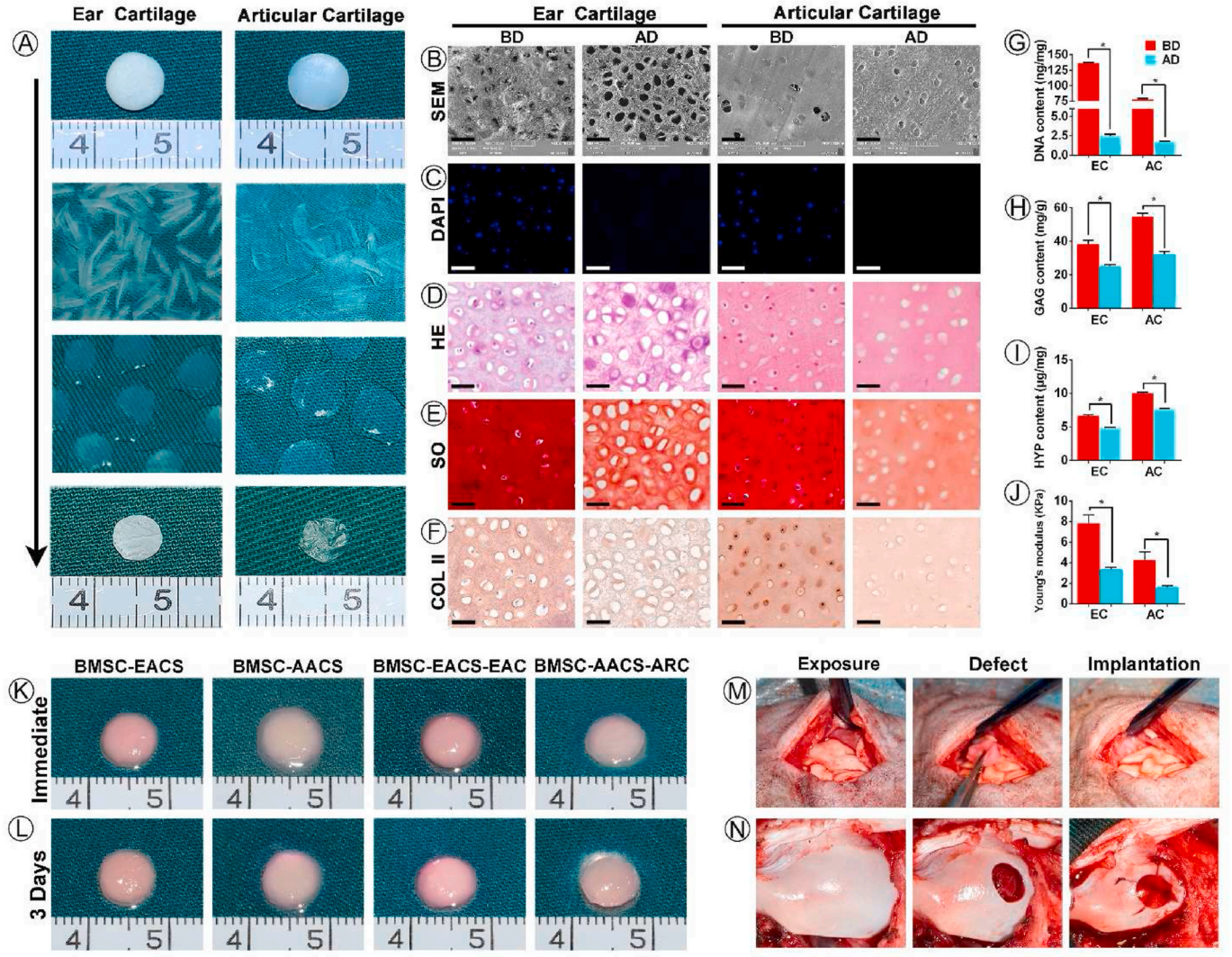

Fig. 2. Preparation of ACSs, cell-ACS constructs, and implantation into native cartilage niches. (A) Preparation of ear and articular ACSs via the procedures of frozen sectioning, decellularization, spreading and lyophilization of ear and articular cartilage. (B) SEM, (C) DAPI staining, (D) HE staining, (E) SO staining and (F) COL II staining of ear and articular cartilage sheet before and after decellularization. Quantitative analysis of (G) DNA content, (H) GAG content, (I) HYP content, and (J) Young's modulus of scaffolds before and after decellularization. (J) Four types of cell-ACS constructs were prepared using the sandwich model. (K) After culturing *in vitro* for 3 days, these constructs were implanted into the (L) ear cartilage or (M) articular cartilage niche. Abbreviations: ACSs, acellular cartilage sheets; BD, before decellularization; AD, after decellularization; SEM, scanning electron microscopy; DAPI, 4′,6-diamidino-2-phenylindole; HE, hematoxylin and eosin; SO, Safranin O; COL II, Collagen II; GAG, Glycosaminoglycan; HYP, Hydroxyproline; EACS, ear acellular cartilage sheet; AACS, articular acellular cartilage sheet; EAC, ear chondrocyte; ARC, articular chondrocyte. Scale bar = 50 μm *p < 0.05.

3.2. Biocompatibility of the ACSs

Biocompatibility is a prerequisite for evaluating whether scaffolds can be used as suitable carriers for seeding cells. The cell seeding efficiency of BMSCs, EAC and ARC in ACS scaffolds was more than 80% (Fig S1B), and these cells adhered well in EACS and AACS after seeding cells on scaffolds for 3 days (Fig S1C). The Live & Dead staining showed that the both BMSCs and chondrocytes survived well in EACS and AACS at 1, 4, and 7 days after cell seeding, and there was an increase in cell number with increasing culture time (Fig S2). These results indicated that both EACS and AACS had good biocompatibility and thus were appropriate for cell seeding, viability, and proliferation.

3.3. Labeling of BMSCs

The lentiviral transfection characteristics of BMSCs, indicated by transfection efficiency, and the effect of the transfection process on the activity of BMSCs, were investigated. The determination of these characteristic is a prerequisite for the follow-up tracking of BMSCs in regenerated tissues and analyzing the regulation of the type of BRC by specific types of cartilage niches. Confocal laser scanning microscopy analysis showed that GFP-positive BMSCs were observed after incubating BMSCs with lentivirus for 24 h (Fig S3A–C), and almost all the BMSCs expressed GFP after the resistance screening with puromycin for 96 h (Fig S3D–F). Moreover, flow cytometry analysis confirmed that GFP-positive BMSCs consisted of 91.6% of all transfected cells (Fig S3G). Meanwhile, the proliferation curve did not demonstrate any significant difference between the labeled and unlabeled cells, which indicated that the labeling did not affect the proliferation characteristics of BMSCs (Fig S3H). These results indicated that the current method could efficiently label BMSCs without affecting their viability, therefore the method was used in subsequent experiments.

3.4. Regulation of the types of BRC by native cartilage niches

This study primary aimed to examine whether specific cartilage

niches could regulate BMSCs to regenerate specific types of cartilage following the preparation of ACSs and labeling of BMSCs. BMSC-EACS and BMSC-AACS constructs were prepared using the sandwich model, which formed a cylinder-shaped cell sheet with a diameter of approximately 7 mm and a thickness of approximately 1 mm (Fig. 2K). The BMSC-AACS construct was more transparent than the BMSC-EACS construct, consistent with the gross differences observed between the two types of ACSs. After 3 days of *in vitro* culture (Fig 2L), the constructs were directly implanted into the *in situ* native ear and articular cartilage niches that were matched with the type of ACSs for 1 year (Figure 2M, N). As shown in Fig. 3, white cartilage-like tissue was formed between native ear cartilages, as demonstrated by the gross image (Fig. 3B). To confirm whether the regenerated tissue was cartilage and whether it was regenerated by the implanted GFP-positive BMSCs, we first detected the expression of GFP and then performed HE staining. Our results showed that GFP-positive cells were traced in the regenerated cartilage with typical lacuna structures, whereas no GFP-positive cells were detected in the native cartilage (Fig. 3C), indicating that GFP-positive cells represented the implanted BMSCs. In addition, histological analysis revealed that the BRC displayed cartilage-specific ECM deposition, as indicated

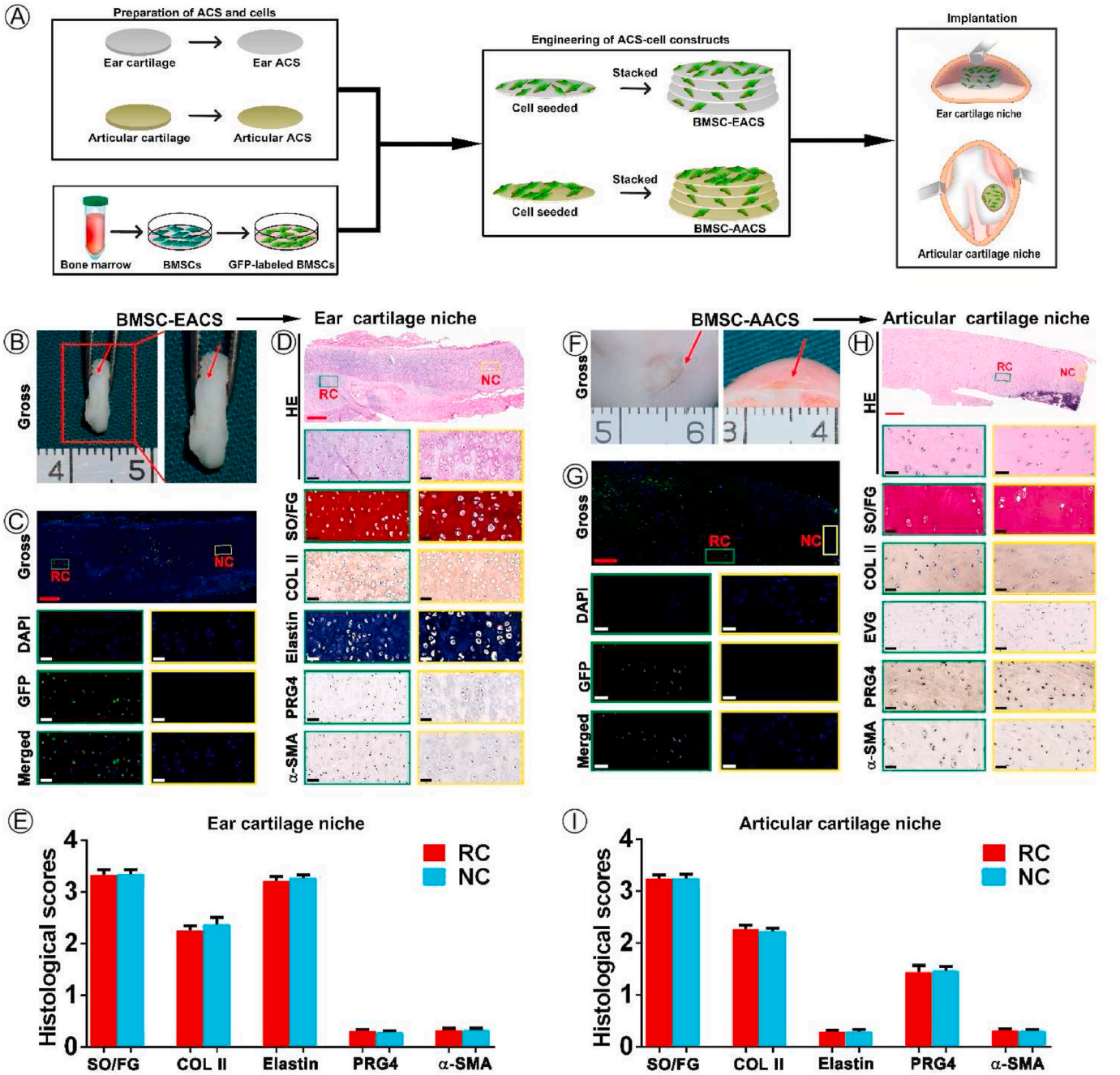

Fig. 3. Regulation of the type of BRC by native ear and articular cartilage niches. (A) Schematic experimental design used to obtain data presented in (B–I). (B–E) Analysis of the effect of native ear cartilage niche on the type of BRC including (B) gross view of BMSC regenerated tissue, (C) GFP-positive cell tracing, (D) histological identification of specific types of cartilage, and (E) quantification analysis of histological staining. (F–I) Analysis of the effect of native articular cartilage niche on the type of BRC including (F) gross view, (G) GFP-positive cell tracing, (H) histological identification of specific types of cartilage, and (I) quantification analysis of histological staining results. Abbreviations: BRC, BMSC regenerated cartilage; RC, regenerated cartilage; NC, native cartilage; PRG4, Proteoglycan 4; α-SMA, alpha-smooth muscle actin. Red scale bar = 500 μm, white and black scale bar = 50 μm.

by the positive staining of SO/FG and COL II (Fig. 3D). Analysis of cartilage-type-specific indicators showed that the BRC demonstrated a high expression of elastin but did not express PRG4 and α-SMA. These results were consistent with the expression patterns observed in native ear cartilage (Fig. 3D). Furthermore, the staining intensity and the extent of positive staining were quantified to score the protein expression of BRC and native cartilage using ImageJ. Consistent with the results of histological staining, BRC showed a protein expression intensity similar to that of the native ear cartilage, which was evaluated to be positive for SO, COL II, and elastin staining; the evaluation for PRG4 and α-SMA was negative (Fig. 3E). Furthermore, RT-qPCR results confirmed that the expression levels of cartilage-specific genes expressed by BRC were similar to those of native cartilage (Fig. 6).

We then investigated the regulation of the type of BRC by the native articular cartilage niche. According to the current results, after implantation for 1 year, the cartilage defects were completely repaired by cartilage-like tissue from gross view (Fig. 3F). GFP-positive cells were detected in the regenerated cartilage, whereas cells in native cartilage did not express GFP (Fig. 3G). HE staining showed that the regenerated area of BMSCs showed chondrocyte lacuna structures, the size and density of lacuna were similar to those of the native cartilage (Fig. 3H). Meanwhile, histological examination (Fig. 3H) and scoring (Fig. 3I)

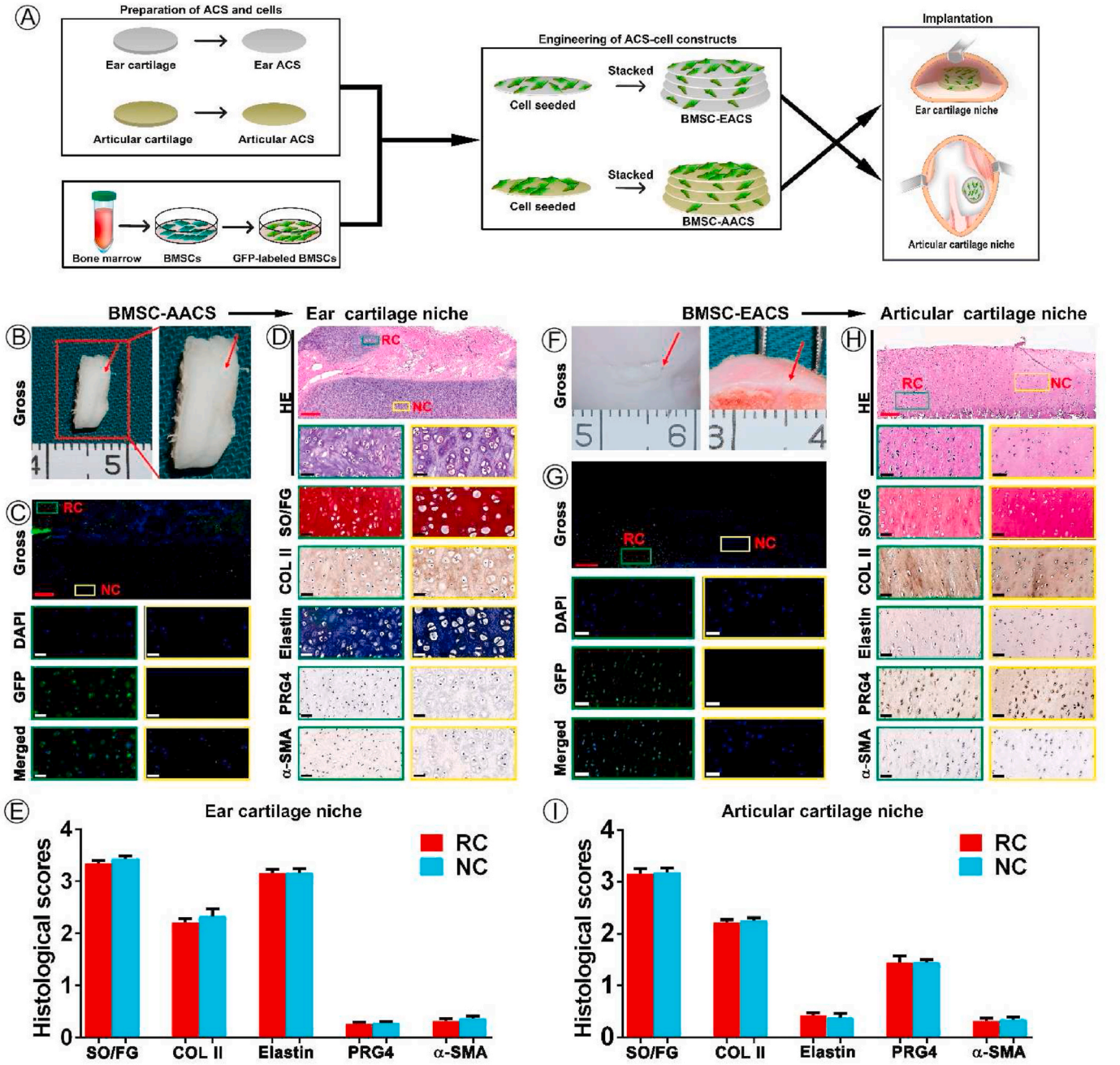

Fig. 4. Effect of ACS provided niche on the regulation of the type of BRC by native cartilage niches. (A) Schematic experimental design used to obtain data presented in (B–I). (B–E) Analysis of effect of native ear cartilage niche on the type of BRC including (B) gross view of BRC, (C) GFP-positive cells tracing, (D) histological identification of specific types of cartilage, and (E) quantification analysis of histological staining. (F–I) Analysis of effect of native articular cartilage niche on the type of BRC including (F) gross view of BRC, (G) GFP-positive cells tracing, (H) histological identification of specific types of cartilage, and (I) quantification analysis of the results of histological staining. Red arrows indicate the regenerated cartilage. Abbreviations: RC, regenerated cartilage; NC, native cartilage. Red scale bar = 500 μm; white and black scale bar = 50 μm.

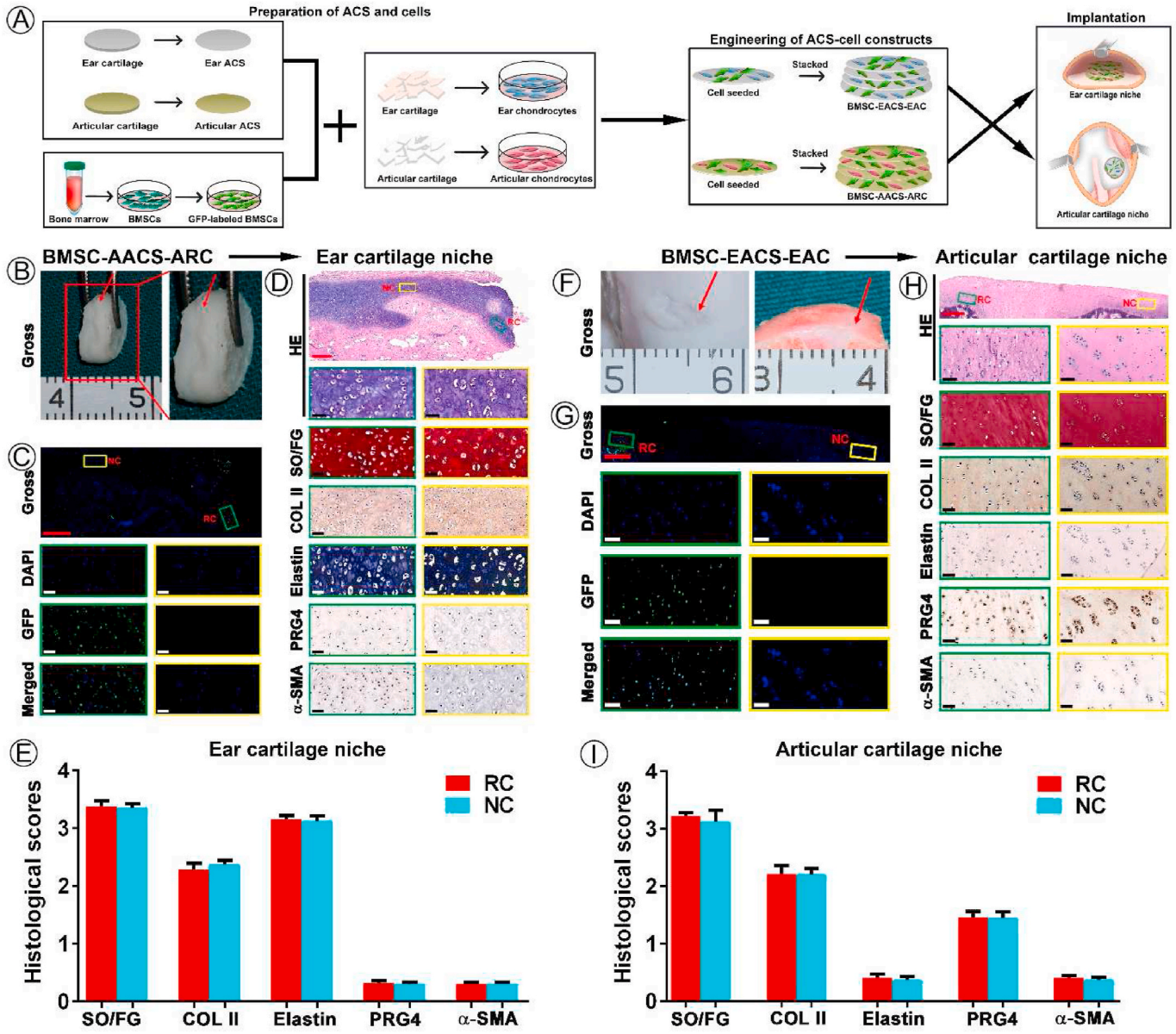

Fig. 5. Effect of mismatched biomimetic cartilage niche on the regulation of native cartilage niches on the type of BRC. (A) Schematic experimental design for data presented in (B–I). (B–E) Analysis of the effect of native ear cartilage niche on the type of BRC including (B) gross view of BRC, (C) GFP-positive cell tracing, (D) histological identification of specific types of cartilage, and (E) quantification analysis of histological staining. (F–I) Analysis of effect of native articular cartilage niche on the type of BRC including (F) gross view of BRC, (G) GFP-positive cell tracing, (H) histological identification of specific types of cartilage, and (I) quantification analysis of histological staining. Red arrows indicate the regenerated cartilage. Abbreviations: RC, regenerated cartilage; NC, native cartilage. Red scale bar = 500 μm; white and black scale bar = 50 μm.

confirmed that the regenerated area of BMSCs displayed cartilage ECM deposition, as indicated by positive staining of SO/FG and COL II. To finally confirm the type of BRC, three types of cartilage-specific markers were analyzed histologically. Our results showed that the cartilage regenerated by BMSCs was consistent with the type of native articular cartilage, which was reflected by positive staining of PRG4 and negative staining of elastin and α-SMA (Fig. 3H). Staining scoring (Fig. 3I) and RT-qPCR (Fig. 6) results showed that the expression levels of SO, COL II, elastin, PRG4, and α-SMA were more comparable in the BRC than those in the native articular cartilage. These results indicated that native ear and articular cartilage niches were capable of regulating BMSC regeneration of elastic and hyaline cartilage, respectively, which was consistent with the cartilage type of the implanted site.

3.5. Effect of the niche contributed by the mismatched scaffold on the regulation of the type of BRC mediated by the native cartilage niche

The second key issue of our study was to check whether the regulation of native cartilage niches on the types of BRC would be affected when the scaffolds did not match the native cartilage niche at the implanted site. BMSC-AACS constructs were implanted into the native ear cartilage niche, and BMSC-EACS constructs were implanted into native articular cartilage niche. Following the culturing of BMSC-AACS constructs in the native ear cartilage niche for 1 year, confocal microscopy (Fig. 4C) and histological examination (Fig. 4D) showed that GFP-positive cells were only traced in the regenerated cartilage. The regenerated cartilage not only showed typical chondrocyte structures, but also demonstrated cartilage-specific ECM. Strong positive staining of elastin and negative staining of PRG4 and α-SMA was observed in BRC and

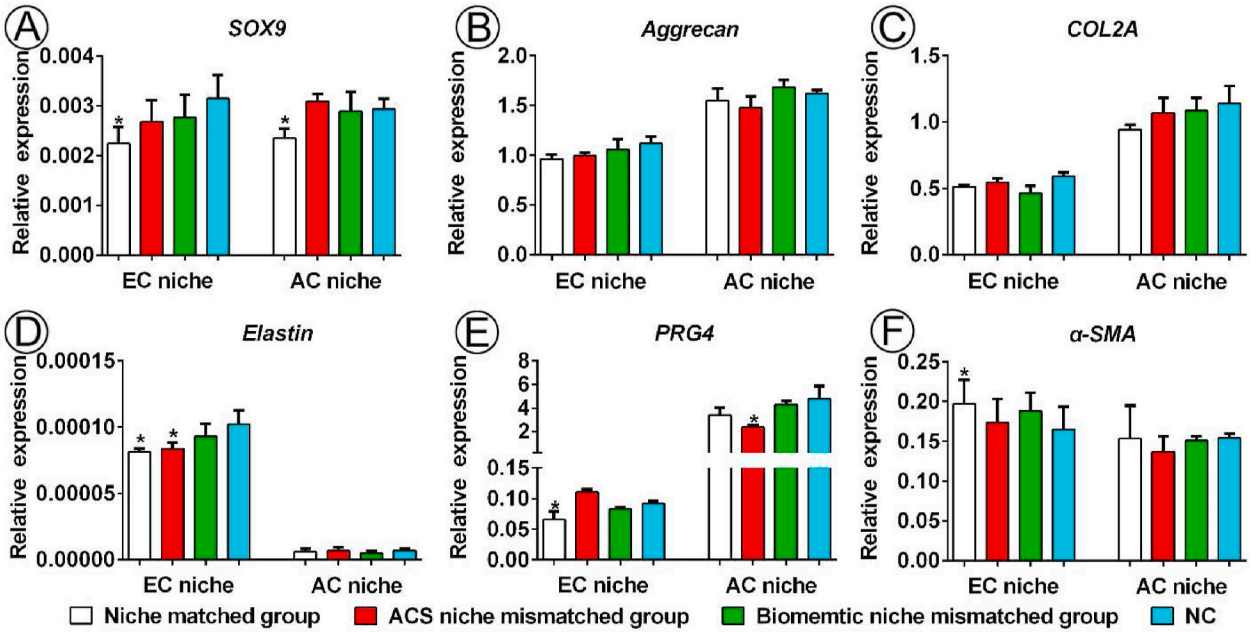

Fig. 6. RT-qPCR analysis of BRC. Determination of the expression of cartilage-related genes (*SOX9*, *aggrecan*, and *COL2A*) and genes associated with specific types of cartilage (*elastin*, *PRG4,* and *α-SMA*) via RT-qPCR using β-actin as the reference gene. The expression level of each gene in RC was compared with that of the NC. Abbreviation: EC, ear cartilage; AC, articular cartilage; NC, native cartilage. *$p < 0.05$.

native ear cartilage (Fig. 4D and E), which was consistent with the expression trends observed at the gene level (Fig. 6). These results indicate that BMSCs formed elastin cartilage.

Next, the type of BRC was evaluated after implantation of BMSC-EACS constructs in the articular cartilage niche for 1 year. As shown in Fig. 4F, cartilage-like tissue formed in the articular cartilage defect. Cell tracing and histological analysis showed that GFP-positive cells were distributed in the regenerated cartilage area (Fig. 4G) and the BRC shared similar specific protein expression levels to those of native articular cartilage at the protein and mRNA levels (Fig. 4H and I; Fig. 6).

3.6. Effect of mismatched biomimetic cartilage niche constructed by ACSs and chondrocytes on the regulation of the BRC's type by native cartilage niches

The final problem to be solved was to check the *in vivo* ultimate regenerated cartilage type of BMSCs when more biomimetic cartilage niche conflicts with native cartilage niche, which will further confirm whether native cartilage niche is indeed the determining factor of the type of BRC. BMSC-AACS-ARC constructs were implanted into the native ear cartilage niche, and ivory white tissue that appeared similar to the surrounding native cartilage was formed after culturing for 1 year (Fig. 5B). Confocal microscopy showed that regenerated tissue expressed GFP-positive cells, whereas the surrounding native cartilage did not (Fig. 5C), indicating the GFP-positive cells represented implanted labeled BMSCs. As shown in Fig. 5D, mature cartilage with typical lacunae and cartilage -specific ECM (GAG and collagen II) deposition was formed in the GFP-positive region. Simultaneously, the analysis of the characteristic proteins of specific types of cartilage showed that the GFP-positive region demonstrated the expression patterns of the native ear cartilage, as indicated by positive staining for elastin and negative staining for PRG4 and α-SMA (Fig. 5D). In addition, the expression levels of cartilage-specific proteins for regenerated cartilage were similar to those for the native ear cartilage (Fig.s. 5E and 6).

Meanwhile, BMSC-EACS-EAC constructs were implanted into the native articular cartilage niche and cultured for 1 year. Our results showed that GFP-positive cells were traced in the regenerated cartilage (Fig. 5G) with typical lacuna structures and cartilage ECM deposition (Fig. 5H), which indicated that BMSCs formed the cartilage-like tissue. Moreover, the same cartilage type-specific protein expression characteristics as those for native articular cartilage were detected in BRC, as observed by the positive staining of PRG4 and negative staining of elastin and α-SMA (Fig. 5H and I).

Notably, as shown in Figure S4, not only the area of BRC, but the entire area of the regenerated cartilage area of the two groups expressed homogeneous cartilage that was consistent with the type of cartilage at the implanted site. Theoretically, the area of the regenerated cartilage contains the implanted ear or articular chondrocytes, which differ from the type of chondrocytes found at the implanted site. Taken together, our results confirmed that native ear and articular cartilage niche determine the differentiation fate and ultimate regenerated cartilage type of implanted BMSCs and chondrocytes.

4. Discussion

BMSCs have been considered the ideal seed cells for tissue-engineered cartilage regeneration [8,48]. However, few studies have reported how to regulate BMSCs to regenerate a specific type of cartilage, which severely limits clinical translation of BRC. The current study demonstrated that *in situ* ear and articular cartilage niches were able to regulate BMSC regeneration of elastic and hyaline cartilage, respectively, which was consistent with the cartilage type of the implanted site. Moreover, the results also confirmed that when the niche provided by ACSs was different from that of the native cartilage niches at the implantation site, the native cartilage niches continued to determine the type of cartilage regenerated from the implanted BMSCs. Most importantly, when the biomimetic cartilage niche constructed by specific types of ACSs and specific types of chondrocytes conflicts with that of the implanted site, the regenerated cartilage types of BMSCs and even the implanted chondrocytes were determined by the native cartilage niche of the implanted site. Collectively, these results confirmed that the *in situ* cartilage niche is the most crucial factor that determines the differentiation fate of BMSCs and the type of regenerated cartilage. The current study provides sufficient evidence and theoretical basis for specific types of cartilage regeneration using chondrogenic potential cells, such as mesenchymal stem cells and chondrocytes.

A suitable scaffold vector for fixing BMSCs at the implanted sites is a prerequisite for examining the regulation of the type of BRC by native cartilage niche. After all, BMSCs harvested without a scaffold vector failed to fix in the implanted *in situ* niche and easily flowed away, making it impossible to track the implanted BMSCs and analyze the type of regenerated cartilage. Currently, many types of synthetic and natural scaffolds with good cell adhesion properties are currently used for cartilage regeneration [49–51]. However, none of them can provide BMSCs with specific biomimetic ECM niches that match different types of *in situ* cartilage niches, because they do not possess the specific structures and components of specific types of cartilage. Therefore, an ideal scaffold that can form a biomimetic cartilage niche matching with the *in situ* niche of the implanted site is still required. ACSs derived from natural cartilage exhibit cartilage components, good cell adhesion functions, and the preservation of the topological structures of cartilage [29,30]. Consistent with the results of our previous study, the current results indicated that ear and articular ACSs not only partially retained GAG and COL II expression but also preserved the inherent specific topological structure of the ear and articular cartilage. Moreover, ACSs were advantageous for cell adhesion and cell proliferation. Particularly, our results confirmed that BMSCs seeded on ACSs could be fixed at the implantation site and were capable of regenerating specific types of cartilage after implantation for 1 year. Taken altogether, the aforementioned characteristics render ACSs ideal scaffolds for the accurate examination of the types of BRC regulated by the native cartilage niche *in situ*.

After the scaffolds were confirmed, we primarily aimed to examine whether the *in situ* specific cartilage niches could regulate BMSCs to regenerate specific types of cartilage. Previous studies have demonstrated that BMSC-scaffold constructs can repair articular cartilage defects and even achieve the regeneration of hyaline-like cartilage [27,28]. However, owing to the lack of cell tracking and identification of characteristic indicators of other types of cartilage, the final regenerated cartilage type of BMSCs remained uncertain. In addition, the understanding of the regulatory role of other types of cartilage niches with respect to the types of BRC are insufficient. Therefore, in this study, GFP-labeled BMSCs were seeded on two types of ACSs and implanted into corresponding types of native cartilage niches in order to accurately investigate the regulation of the type of BRC mediated by different types of native cartilage niches. Our results demonstrated that the tracked GFP-positive BMSCs in the native ear cartilage niche formed mature elastic cartilage; the nature of the regenerated cartilage was confirmed by the strong positive staining of elastin (specific protein of elastin cartilage) and negative staining of PRG4 (specific protein of articular cartilage) and α-SMA (specific protein of fibrocartilage). Furthermore, BMSCs in the native articular cartilage niche regenerated hyaline cartilage, consistent with the implanted niche *in situ*, as evidenced by the expression of PRG4 but not that of elastin and α-SMA. Although it is still unclear how the native cartilage niche regulates the regeneration of specific types of cartilage by BMSCs, we speculate that this is the result of the combined effects of the following factors:1) the native ear and articular cartilage niches are natural sites for the growth and development of the ear and articular cartilage, respectively, which exhibit specific biomechanics, growth factors, nutrients, and physical parameters (i.e., matrix rigidity, shear stress, and oxygen tension) required for the regeneration of different types of cartilages [52–55]; 2) the extracellular vesicles secreted by native chondrocytes may play a major role in BMSC–chondrocyte communication, thereby promoting the functional differentiation and matrix production of BMSCs [56]; and 3) ACSs and the sandwich model provide a local cartilaginous niche for BMSCs; hence, BMSCs are constantly stimulated by the cartilage niche. Collectively, these results confirmed that the cartilage niche at the site of implantation formed by specific types of ACSs and specific types of native cartilage niche determine the type of regenerated cartilage by BMSCs, consistent with the type of cartilage at the implantation site.

However, whether the regulation of the types of BRC by the native niches is affected when the scaffolds do not match the native cartilage niche at the implanted site is also of considerable concern. Notably, scaffolds exhibit unique characteristics for regulating the chondrogenic differentiation of stem cells due to the diversity of structures and tissue-specific compositions [57–60]. To explore the dominant factors responsible for regulating cartilage-specific differentiation of BMSCs, in the current study, BMSCs were seeded on the ear and articular ACSs using the sandwich model, and implanted into the native articular and ear cartilage sites that did not match the types of ACSs and cultured for 1 year. Our findings demonstrated that in this case, native ear and articular cartilage niches could still regulate BMSCs to regenerate elastin and hyaline cartilage, respectively. These results indicated that the type of ACS did not affect the determinative role of the *in situ* native niche on the type of BRC. In other words, the native cartilage niche continued to be the dominant factor for regulating the type of cartilage regenerated by BMSCs.

Nevertheless, the different types of cartilage niches formed by ACS alone were limited, and hence, were insufficient to counter the regulation of the types of BRC mediated by the native cartilage niche. This study finally examined whether the type of cartilage regenerated by BMSCs was still determined by the native niche if biomimetic cartilage niches conflicted with native cartilage niches. It is known that chondrocytes can create a more biomimetic chondrogenic niche for BMSCs by secreting soluble growth factors and cartilage ECM components [61,62]. Previous studies have also confirmed that BMSCs can achieve cartilage regeneration *in vitro* upon co-culturing with chondrocytes and the reverse ossification of BMSCs can be observed in a subcutaneous environment for stable cartilage regeneration upon co-transplantation with chondrocytes [22,61,63,64]. Consequently, the combination of specific types of chondrocytes with specific types of ACSs could provide a more biomimetic cartilage niche for BMSCs. Therefore, a further examination of the cartilage types regenerated by BMSCs in case of the conflict of biomimetic cartilage niches with different types of native niches is required. The current study showed that the type of cartilage regenerated by tracked GFP-positive BMSC continued to be determined by the native cartilage niche at the implanted site rather than the biomimetic cartilage niche formed by ACS and chondrocytes. Furthermore, the entire regenerated area demonstrated the formation of homogeneous cartilage that was consistent with the type of native cartilage niche at the implantation site, implying that the chondrocytes underwent transdifferentiation [65,66] and regenerated cartilage that was consistent with the native cartilage niche. Taken together, our results further confirmed that the native cartilage niche determines the differentiation fate and type of the cartilage regenerated by implanted cells with chondrogenic potential, including stem cells and chondrocytes.

5. Conclusion

In summary, the current study demonstrated that the *in situ* native cartilage niche is the determining factor for the ultimate regenerated cartilage type of stem cells as well as chondrocytes. It can regulate the directional differentiation of stem cells and transdifferentiation of chondrocytes to regenerate a specific type of cartilage consistent with the native niche. Although the transition process and molecular mechanisms underlying differentiation and the regeneration of specific types of cartilages mediated by BMSCs need to be elucidated, our results provide sufficient evidence and a theoretical basis for the regeneration of specific types of cartilages using cells with chondrogenic potential, such as mesenchymal stem cells and chondrocytes.

CRediT authorship contribution statement

Mengjie Hou: Conceptualization, Data curation, Formal analysis, Writing – original draft. **Baoxing Tian:** Data curation, Formal analysis, Methodology. **Baoshuai Bai:** Data curation, Formal analysis, Validation. **Zheng Ci:** Data curation. **Yu Liu:** Supervision. **Yixin Zhang:**

Supervision. **Guangdong Zhou:** Conceptualization, Funding acquisition, Supervision, Writing – review & editing. **Yilin Cao:** Conceptualization, Funding acquisition, Supervision, Writing – review & editing.

Declaration of competing interest

The authors declare no potential conflicts of interest.

Acknowledgments

This research was supported by the National Key Research and Development Program of China (2017YFC1103900), the National Natural Science Foundation of China (81671837, 81871502), the Shanghai Collaborative Innovation Program on Regenerative Medicine and Stem Cell Research (2019CXJQ01), and Clinical Research Plan of SHDC (SHDC2020CR2045B).

Appendix A. Supplementary data

Supplementary data to this article can be found online at https://doi.org/10.1016/j.bioactmat.2021.11.007.

Data availability statement

The data within the paper that support the findings of this study are available on request from the corresponding author.

References

[1] A.J. Fosang, F. Beier, Emerging Frontiers in cartilage and chondrocyte biology, Best Pract. Res. Clin. Rheumatol. 25 (6) (2011) 751–766, https://doi.org/10.1016/j.berh.2011.11.010.
[2] R. Langer, J.P. Vacanti, Tissue engineering, Science 260 (5110) (1993) 920, https://doi.org/10.1126/science.8493529.
[3] P. Gentile, M.G. Scioli, A. Bielli, A. Orlandi, V. Cervelli, Reconstruction of alar nasal cartilage defects using a tissue engineering technique based on a combined use of autologous chondrocyte micrografts and platelet-rich plasma: preliminary clinical and instrumental evaluation, plastic and reconstructive surgery, Global open 4 (10) (2016) e1027, https://doi.org/10.1097/GOX.0000000000001027.
[4] C. Chung, J.A. Burdick, Engineering cartilage tissue, Adv. Drug Deliv. Rev. 60 (2) (2008) 243–262, https://doi.org/10.1016/j.addr.2007.08.027.
[5] G. Ceccarelli, P. Gentile, M. Marcarelli, M. Balli, F.L. Ronzoni, L. Benedetti, M. G. Cusella De Angelis, In vitro and in vivo studies of alar-nasal cartilage using autologous micro-grafts: the use of the Rigenera®Protocol in the treatment of an osteochondral lesion of the nose, Pharmaceuticals 10 (2) (2017), https://doi.org/10.3390/ph10020053.
[6] A. Bielli, M.G. Scioli, P. Gentile, V. Cervelli, A. Orlandi, Adipose-derived stem cells in cartilage regeneration: current perspectives, Regen. Med. 11 (2016), https://doi.org/10.2217/rme-2016-0077.
[7] J. Ding, B. Chen, T. Lv, X. Liu, X. Fu, Q. Wang, L. Yan, N. Kang, Y. Cao, R. Xiao, Bone marrow mesenchymal stem cell-based engineered cartilage ameliorates polyglycolic acid/polylactic acid scaffold-induced inflammation through M2 polarization of macrophages in a pig model, Stem cells translational medicine 5 (8) (2016) 1079–1089, https://doi.org/10.5966/sctm.2015-0263.
[8] P.K. Gupta, A.K. Das, A. Chullikana, A.S. Majumdar, Mesenchymal stem cells for cartilage repair in osteoarthritis, Stem Cell Res. Ther. 3 (4) (2012) 25, https://doi.org/10.1186/scrt116.
[9] M. Mazor, E. Lespessailles, R. Coursier, R. Daniellou, T.M. Best, H. Toumi, Mesenchymal stem-cell potential in cartilage repair: an update, J. Cell Mol. Med. 18 (12) (2014) 2340–2350, https://doi.org/10.1111/jcmm.12378.
[10] M.F. Pittenger, A.M. Mackay, S.C. Beck, R.K. Jaiswal, R. Douglas, J.D. Mosca, M. A. Moorman, D.W. Simonetti, S. Craig, D.R. Marshak, Multilineage potential of adult human mesenchymal stem cells, Science 284 (5411) (1999) 143, https://doi.org/10.1126/science.284.5411.143.
[11] A. Naumann, J.E. Dennis, A. Awadallah, D.A. Carrino, J.M. Mansour, E. Kastenbauer, A.I. Caplan, Immunochemical and mechanical characterization of cartilage subtypes in rabbit, J. Histochem. Cytochem. 50 (8) (2002) 1049–1058, https://doi.org/10.1177/002215540205000807.
[12] L. Zhang, M. Spector, Comparison of three types of chondrocytes in collagen scaffolds for cartilage tissue engineering, Biomed. Mater. 4 (4) (2009), 045012, https://doi.org/10.1088/1748-6041/4/4/045012.
[13] K.E. Sayed, A. Haisch, T. John, U. Marzahn, A. Lohan, R.D. Müller, B. Kohl, W. Ertel, K. Stoelzel, G. Schulze-Tanzil, Heterotopic autologous chondrocyte Transplantation—A realistic approach to support articular cartilage repair? Tissue Eng. B Rev. 16 (6) (2010) 603–616, https://doi.org/10.1089/ten.teb.2010.0167.
[14] M. Mizuno, T. Takebe, S. Kobayashi, S. Kimura, M. Masutani, S. Lee, Y.H. Jo, J. I. Lee, H. Taniguchi, Elastic cartilage reconstruction by transplantation of cultured hyaline Cartilage—Derived chondrocytes, Trans. Pap. 46 (4) (2014) 1217–1221, https://doi.org/10.1016/j.transproceed.2013.12.006.
[15] S.M. Mithieux, A.S. Weiss, Elastin, Advances in Protein Chemistry, Academic Press, 2005, pp. 437–461.
[16] J.C. Rodríguez-Cabello, I. González de Torre, A. Ibañez-Fonseca, M. Alonso, Bioactive scaffolds based on elastin-like materials for wound healing, Adv. Drug Deliv. Rev. 129 (2018) 118–133, https://doi.org/10.1016/j.addr.2018.03.003.
[17] T. Matsuzaki, O. Alvarez-Garcia, S. Mokuda, K. Nagira, M. Olmer, R. Gamini, K. Miyata, Y. Akasaki, A.I. Su, H. Asahara, M.K. Lotz, FoxO transcription factors modulate autophagy and proteoglycan 4 in cartilage homeostasis and osteoarthritis, Sci. Transl. Med. 10 (428) (2018), https://doi.org/10.1126/scitranslmed.aan0746 eaan0746.
[18] S.Y. Lee, T. Niikura, A.H. Reddi, Superficial zone protein (lubricin) in the different tissue compartments of the knee joint: modulation by transforming growth factor beta 1 and interleukin-1 beta, Tissue Eng. 14 (11) (2008) 1799–1808, https://doi.org/10.1089/ten.tea.2007.0367.
[19] A. Lawrence, X. Xu, M.D. Bible, S. Calve, C.P. Neu, A. Panitch, Synthesis and characterization of a lubricin mimic (mLub) to reduce friction and adhesion on the articular cartilage surface, Biomaterials 73 (2015) 42–50, https://doi.org/10.1016/j.biomaterials.2015.09.012.
[20] M. Keeney, J.H. Lai, F. Yang, Recent progress in cartilage tissue engineering, Curr. Opin. Biotechnol. 22 (5) (2011) 734–740, https://doi.org/10.1016/j.copbio.2011.04.003.
[21] Y.Y. Li, T.H. Choy, F.C. Ho, P.B. Chan, Scaffold composition affects cytoskeleton organization, cell-matrix interaction and the cellular fate of human mesenchymal stem cells upon chondrogenic differentiation, Biomaterials 52 (2015) 208–220, https://doi.org/10.1016/j.biomaterials.2015.02.037.
[22] K. Liu, G.D. Zhou, W. Liu, W.J. Zhang, L. Cui, X. Liu, T.Y. Liu, Y. Cao, The dependence of in vivo stable ectopic chondrogenesis by human mesenchymal stem cells on chondrogenic differentiation in vitro, Biomaterials 29 (14) (2008) 2183–2192, https://doi.org/10.1016/j.biomaterials.2008.01.021.
[23] Y.-N. Wu, Z. Yang, J.H.P. Hui, H.-W. Ouyang, E.H. Lee, Cartilaginous ECM component-modification of the micro-bead culture system for chondrogenic differentiation of mesenchymal stem cells, Biomaterials 28 (28) (2007) 4056–4067, https://doi.org/10.1016/j.biomaterials.2007.05.039.
[24] X. Hu, Y. Wang, Y. Tan, J. Wang, H. Liu, Y. Wang, S. Yang, M. Shi, S. Zhao, Y. Zhang, Q. Yuan, A difunctional regeneration scaffold for knee repair based on aptamer-directed cell recruitment, Adv. Mater. 29 (15) (2017) 1605235, https://doi.org/10.1002/adma.201605235.
[25] R.L. Dahlin, L.A. Kinard, J. Lam, C.J. Needham, S. Lu, F.K. Kasper, A.G. Mikos, Articular chondrocytes and mesenchymal stem cells seeded on biodegradable scaffolds for the repair of cartilage in a rat osteochondral defect model, Biomaterials 35 (26) (2014) 7460–7469, https://doi.org/10.1016/j.biomaterials.2014.05.055.
[26] J. Xue, A. He, Y. Zhu, Y. Liu, D. Li, Z. Yin, W. Zhang, W. Liu, Y. Cao, G. Zhou, Repair of articular cartilage defects with acellular cartilage sheets in a swine model, Biomed. Mater. 13 (2) (2018), 025016, https://doi.org/10.1088/1748-605X/aa99a4.
[27] Y. Sun, Y. You, W. Jiang, B. Wang, Q. Wu, K. Dai, 3D bioprinting dual-factor releasing and gradient-structured constructs ready to implant for anisotropic cartilage regeneration, Sci Adv 6 (2020), https://doi.org/10.1126/sciadv.aay1422.
[28] H. Kang, Y. Zeng, S. Varghese, Functionally graded multilayer scaffolds for in vivo osteochondral tissue engineering, Acta Biomater. 78 (2018) 365–377, https://doi.org/10.1016/j.actbio.2018.07.039.
[29] Y.Y. Gong, J.X. Xue, W.J. Zhang, G.D. Zhou, W. Liu, Y. Cao, A sandwich model for engineering cartilage with acellular cartilage sheets and chondrocytes, Biomaterials 32 (9) (2011) 2265–2273, https://doi.org/10.1016/j.biomaterials.2010.11.078.
[30] J.X. Xue, Y.Y. Gong, G.D. Zhou, W. Liu, Y. Cao, W.J. Zhang, Chondrogenic differentiation of bone marrow-derived mesenchymal stem cells induced by acellular cartilage sheets, Biomaterials 33 (24) (2012) 5832–5840, https://doi.org/10.1016/j.biomaterials.2012.04.054.
[31] G. Zhou, H. Jiang, Z. Yin, Y. Liu, Q. Zhang, C. Zhang, B. Pan, J. Zhou, X. Zhou, H. Sun, D. Li, A. He, Z. Zhang, W. Zhang, W. Liu, Y. Cao, In vitro regeneration of patient-specific ear-shaped cartilage and its first clinical application for auricular reconstruction, EBioMedicine 28 (2018) 287–302, https://doi.org/10.1016/j.ebiom.2018.01.011.
[32] J. Chen, Z. Yuan, Y. Liu, R. Zheng, Y. Dai, R. Tao, H. Xia, H. Liu, Z. Zhang, W. Zhang, W. Liu, Y. Cao, G. Zhou, Improvement of in vitro three-dimensional cartilage regeneration by a novel hydrostatic pressure bioreactor, Stem cells translational medicine 6 (3) (2017) 982–991, https://doi.org/10.5966/sctm.2016-0118.
[33] G. Kesava Reddy, C.S. Enwemeka, A simplified method for the analysis of hydroxyproline in biological tissues, Clin. Biochem. 29 (3) (1996) 225–229, https://doi.org/10.1016/0009-9120(96)00003-6.
[34] D. Yan, G. Zhou, X. Zhou, W. Liu, W.J. Zhang, X. Luo, L. Zhang, T. Jiang, L. Cui, Y. Cao, The impact of low levels of collagen IX and pyridinoline on the mechanical properties of in vitro engineered cartilage, Biomaterials 30 (5) (2009) 814–821, https://doi.org/10.1016/j.biomaterials.2008.10.042.
[35] A. Narayanaswamy, M.H. Nai, M.E. Nongpiur, H.M. Htoon, A. Thomas, T. Sangtam, C.T. Lim, T.T. Wong, T. Aung, Young's modulus determination of normal and glaucomatous human Iris, Invest. Ophthalmol. Vis. Sci. 60 (7) (2019) 2690–2695, https://doi.org/10.1167/iovs.18-26455.
[36] C. Rovera, C.A. Cozzolino, M. Ghaani, D. Morrone, R.T. Olsson, S. Farris, Mechanical behavior of biopolymer composite coatings on plastic films by depth-

sensing indentation Б—∫ A nanoscale study, J. Colloid Interface Sci. 512 (2018) 638–646, https://doi.org/10.1016/j.jcis.2017.10.108.
[37] Q. Shang, Z. Wang, W. Liu, Y. Shi, L. Cui, Y. Cao, Tissue-engineered bone repair of sheep cranial defects with autologous bone marrow stromal cells, J. Craniofac. Surg. 12 (6) (2001).
[38] A. Rodriguez, Y.L. Cao, C. Ibarra, S. Pap, M. Vacanti, R.D. Eavey, C.A. Vacanti, Characteristics of cartilage engineered from human pediatric auricular cartilage, Plast. Reconstr. Surg. 103 (4) (1999) 1111–1119, https://doi.org/10.1097/00006534-199904040-00001.
[39] G. Zhou, W. Liu, L. Cui, X. Wang, T. Liu, Y. Cao, Repair of porcine articular osteochondral defects in non-weightbearing areas with autologous bone marrow stromal cells, Tissue Eng. 12 (11) (2006) 3209–3221, https://doi.org/10.1089/ten.2006.12.3209.
[40] J.-M. Escoffre, E. Bellard, M. Golzio, J. Teissié, M.-P. Rols, Transgene expression of transfected supercoiled plasmid DNA concatemers in mammalian cells, J. Gene Med. 11 (11) (2009) 1071–1073, https://doi.org/10.1002/jgm.1384.
[41] C.H. Jin, K. Kusuhara, Y. Yonemitsu, A. Nomura, S. Okano, H. Takeshita, M. Hasegawa, K. Sueishi, T. Hara, Recombinant Sendai virus provides a highly efficient gene transfer into human cord blood-derived hematopoietic stem cells, Gene Ther. 10 (3) (2003) 272–277, https://doi.org/10.1038/sj.gt.3301877.
[42] J. Xue, B. Feng, R. Zheng, Y. Lu, G. Zhou, W. Liu, Y. Cao, Y. Zhang, W.J. Zhang, Engineering ear-shaped cartilage using electrospun fibrous membranes of gelatin/polycaprolactone, Biomaterials 34 (11) (2013) 2624–2631, https://doi.org/10.1016/j.biomaterials.2012.12.011.
[43] A. He, L. Liu, X. Luo, Y. Liu, Y. Liu, F. Liu, X. Wang, Z. Zhang, W. Zhang, W. Liu, Y. Cao, G. Zhou, Repair of osteochondral defects with in vitro engineered cartilage based on autologous bone marrow stromal cells in a swine model, Sci. Rep. 7 (2017) 40489, https://doi.org/10.1038/srep40489.
[44] X. Luo, G. Zhou, W. Liu, W.J. Zhang, L. Cen, L. Cui, Y. Cao, In vitro precultivation alleviates post-implantation inflammation and enhances development of tissue-engineered tubular cartilage, Biomed. Mater. 4 (2) (2009), 025006, https://doi.org/10.1088/1748-6041/4/2/025006.
[45] F. Varghese, A.B. Bukhari, R. Malhotra, A. De, IHC Profiler: an open source plugin for the quantitative evaluation and automated scoring of immunohistochemistry images of human tissue samples, PLoS One 9 (5) (2014), https://doi.org/10.1371/journal.pone.0096801 e96801-e96801.
[46] K.N. Shah, R. Bhatt, J. Rotow, J. Rohrberg, V. Olivas, V.E. Wang, G. Hemmati, M. M. Martins, A. Maynard, J. Kuhn, J. Galeas, H.J. Donnella, S. Kaushik, A. Ku, S. Dumont, G. Krings, H.J. Haringsma, L. Robillard, A.D. Simmons, T.C. Harding, F. McCormick, A. Goga, C.M. Blakely, T.G. Bivona, S. Bandyopadhyay, Aurora kinase A drives the evolution of resistance to third-generation EGFR inhibitors in lung cancer, Nat. Med. 25 (1) (2019) 111–118, https://doi.org/10.1038/s41591-018-0264-7.
[47] F. Li, V.X. Truong, P. Fisch, C. Levinson, V. Glattauer, M. Zenobi-Wong, H. Thissen, J.S. Forsythe, J.E. Frith, Cartilage tissue formation through assembly of microgels containing mesenchymal stem cells, Acta Biomater. 77 (2018) 48–62, https://doi.org/10.1016/j.actbio.2018.07.015.
[48] Y. Wang, M. Yuan, Q.-Y. Guo, S.-B. Lu, J. Peng, Mesenchymal stem cells for treating articular cartilage defects and osteoarthritis, Cell Transplant. 24 (9) (2015) 1661–1678, https://doi.org/10.3727/096368914X683485.
[49] E.A. Kiyotake, E.C. Beck, M.S. Detamore, Cartilage extracellular matrix as a biomaterial for cartilage regeneration, Ann. N. Y. Acad. Sci. 1383 (1) (2016) 139–159, https://doi.org/10.1111/nyas.13278.
[50] C. Zhao, A. Tan, G. Pastorin, H.K. Ho, Nanomaterial scaffolds for stem cell proliferation and differentiation in tissue engineering, Biotechnol. Adv. 31 (5) (2013) 654–668, https://doi.org/10.1016/j.biotechadv.2012.08.001.
[51] J. Iwasa, L. Engebretsen, Y. Shima, M. Ochi, Clinical application of scaffolds for cartilage tissue engineering, Knee Surg. Sports Traumatol. Arthrosc. 17 (6) (2009) 561–577, https://doi.org/10.1007/s00167-008-0663-2.
[52] A.J. Wagers, The stem cell niche in regenerative medicine, Cell Stem Cell 10 (4) (2012) 362–369, https://doi.org/10.1016/j.stem.2012.02.018.
[53] P.M. Gilbert, K.L. Havenstrite, K.E.G. Magnusson, A. Sacco, N.A. Leonardi, P. Kraft, N.K. Nguyen, S. Thrun, M.P. Lutolf, H.M. Blau, Substrate elasticity regulates skeletal muscle stem cell self-renewal in culture, Science (New York, N.Y.) 329 (5995) (2010) 1078–1081, https://doi.org/10.1126/science.1191035.
[54] K.H. Vining, D.J. Mooney, Mechanical forces direct stem cell behaviour in development and regeneration, Nat. Rev. Mol. Cell Biol. 18 (12) (2017) 728–742, https://doi.org/10.1038/nrm.2017.108.
[55] F. Guilak, D.M. Cohen, B.T. Estes, J.M. Gimble, W. Liedtke, C.S. Chen, Control of stem cell fate by physical interactions with the extracellular matrix, Cell Stem Cell 5 (1) (2009) 17–26, https://doi.org/10.1016/j.stem.2009.06.016.
[56] M. Kim, D.R. Steinberg, J.A. Burdick, R.L. Mauck, Extracellular vesicles mediate improved functional outcomes in engineered cartilage produced from MSC/chondrocyte cocultures, Proc. Natl. Acad. Sci. U.S.A. 116 (5) (2019) 1569–1578, https://doi.org/10.1073/pnas.1815447116.
[57] A. Cheng, Z. Schwartz, A. Kahn, X. Li, Z. Shao, M. Sun, Y. Ao, B.D. Boyan, H. Chen, Advances in porous scaffold design for bone and cartilage tissue engineering and regeneration, Tissue Eng. B Rev. 25 (1) (2018) 14–29, https://doi.org/10.1089/ten.teb.2018.0119.
[58] K.E.M. Benders, P.R.v. Weeren, S.F. Badylak, D.l.B.F. Saris, W.J.A. Dhert, J. Malda, Extracellular matrix scaffolds for cartilage and bone regeneration, Trends Biotechnol. 31 (3) (2013) 169–176, https://doi.org/10.1016/j.tibtech.2012.12.004.
[59] C. Wang, W. Huang, Y. Zhou, L. He, Z. He, Z. Chen, X. He, S. Tian, J. Liao, B. Lu, Y. Wei, M. Wang, 3D printing of bone tissue engineering scaffolds, Bioactive materials 5 (1) (2020) 82–91, https://doi.org/10.1016/j.bioactmat.2020.01.004.
[60] M. Yadid, R. Feiner, T. Dvir, Gold nanoparticle-integrated scaffolds for tissue engineering and regenerative medicine, Nano Lett. 19 (4) (2019) 2198–2206, https://doi.org/10.1021/acs.nanolett.9b00472.
[61] X. Liu, H. Sun, D. Yan, L. Zhang, X. Lv, T. Liu, W. Zhang, W. Liu, Y. Cao, G. Zhou, In vivo ectopic chondrogenesis of BMSCs directed by mature chondrocytes, Biomaterials 31 (36) (2010) 9406–9414, https://doi.org/10.1016/j.biomaterials.2010.08.052.
[62] P.M. van der Kraan, P. Buma, T. van Kuppevelt, W.B. van Den Berg, Interaction of chondrocytes, extracellular matrix and growth factors: relevance for articular cartilage tissue engineering, Osteoarthritis Cartilage 10 (8) (2002) 631–637, https://doi.org/10.1053/joca.2002.0806.
[63] L. Zhang, A. He, Z. Yin, Z. Yu, X. Luo, W. Liu, W. Zhang, Y. Cao, Y. Liu, G. Zhou, Regeneration of human-ear-shaped cartilage by co-culturing human microtia chondrocytes with BMSCs, Biomaterials 35 (18) (2014) 4878–4887, https://doi.org/10.1016/j.biomaterials.2014.02.043.
[64] D. Li, L. Zhu, Y. Liu, Z. Yin, Y. Liu, F. Liu, A. He, S. Feng, Y. Zhang, Z. Zhang, W. Zhang, W. Liu, Y. Cao, G. Zhou, Stable subcutaneous cartilage regeneration of bone marrow stromal cells directed by chondrocyte sheet, Acta Biomater. 54 (2017) 321–332, https://doi.org/10.1016/j.actbio.2017.03.031.
[65] J. Hong, E.A. Lee, E.-S. Lee, G. Jung, H. Jeong, H. Lee, H. Lee, N.S. Hwang, Induced myogenic commitment of human chondrocytes via non-viral delivery of minicircle DNA, J. Contr. Release 200 (2015) 212–221, https://doi.org/10.1016/j.jconrel.2014.12.031.
[66] S. Bonakdar, M. Mahmoudi, L. Montazeri, M. Taghipoor, A. Bertsch, M. A. Shokrgozar, S. Sharifi, M. Majidi, O. Mashinchian, M. Hamrang Sekachaei, P. Zolfaghari, P. Renaud, Cell-imprinted substrates modulate differentiation, redifferentiation, and transdifferentiation, ACS Appl. Mater. Interfaces 8 (22) (2016) 13777–13784, https://doi.org/10.1021/acsami.6b03302.